HHS Public Access

Author manuscript

Peptides. Author manuscript; available in PMC 2019 August 01.

Published in final edited form as:

Peptides. 2018 August ; 106: 9–20. doi:10.1016/j.peptides.2018.05.011.

Antibacterial, Antifungal, Anticancer Activities and Structural Bioinformatics Analysis of Six Naturally Occurring Temporins

Biswajit Mishra[a,1], **Xiuqing Wang**[a,b,1], **Tamara Lushnikova**[a], **Yingxia Zhang**[a,c], **Radha M. Golla**[a], **Jayaram Lakshmaiah Narayana**[a], **Chunfeng Wang**[a,d], **Timothy R. McGuire**[e], and **Guangshun Wang**[a,*]

[†]Department of Pathology and Microbiology, College of Medicine, University of Nebraska Medical Center, Omaha, NE 68198-5900, USA

[b]Department of Clinical Medicine, Ningxia Medical University, Yinchuan 750004, Ningxia, China

[c]Key Laboratory of Tropical Biological Resources, Ministry of Education, College of Marine Science, Hainan University, Haikou 570228, Hainan, China

[d]The First Affiliated Hospital of Zhengzhou University, 1 Mianfang Road, Zhengzhou 450052, Henan, China

[e]Department of Pharmacy Practice, University of Nebraska Medical Center, Omaha, NE 68198-6025, USA

Abstract

Antimicrobial peptides are a special class of natural products with potential applications as novel therapeutics. This study focuses on six temporins (four with no activity data and two as positive controls). Using synthetic peptides, we report antibacterial, antifungal, and anticancer activities of temporins-CPa, CPb, 1Ga, 1Oc, 1Ola, and 1SPa. While temporin-1Ga and temporin-1OLa showed higher antifungal and anticancer activity, most of these peptides were active primarily against Gram-positive bacteria. Temporin-1OLa, with the highest cell selectivity index, could preferentially kill methicillin-resistant *Staphylococcus aureus* (MRSA), consistent with a reduced hemolysis in the presence of bacteria. Mechanistically, temporin-1OLa rapidly killed MRSA by damaging bacterial membranes. Using micelles as a membrane-mimetic model, we determined the three-dimensional structure of temporin-1OLa by NMR spectroscopy. The peptide adopted a two-domain structure where a hydrophobic patch is followed by a classic amphipathic helix covering residues P3-I12. Such a structure is responsible for anti-biofilm ability in vitro and in vivo protection of wax moths *Galleria mellonella* from staphylococcal infection. Finally, our bioinformatic analysis leads to a classification of temporins into six types and confers significance to this NMR structure since temporin-1OLa shares a sequence model with 62% of temporins.

[*]Corresponding author. Mailing address: Guangshun Wang, Ph.D., Department of Pathology and Microbiology, University of Nebraska Medical Center, 985900 Nebraska Medical Center, Omaha, NE 68198-5900, USA, Phone: (402) 559-4176; Fax: (402) 559-5900; gwang@unmc.edu.

[1]These two authors made major and comparable contributions to this study.

Collectively, our results indicate the potential of temporin-1OLa as a new anti-MRSA compound, which shows an even better anti-biofilm capability in combination with linezolid.

Graphic abstract

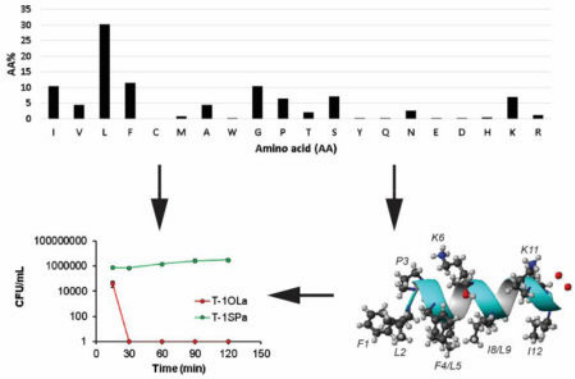

Keywords

Antimicrobial peptides; database; *Galleria mellonella*; MRSA; NMR; *Staphylococcus aureus*; temporin

1. Introduction

Our search for new antimicrobial agents is frequently inspired by nature. Outstanding examples include the discoveries of antibacterial penicillin from fungi in 1928, daptomycin from bacteria in 1986, and antimalarial drug artemisinin (Qinghaosu) from a Chinese herb in the 1960s [1–3]. Our recently increased interest in natural products results from an urgent need for new antibiotics that are capable of eliminating antibiotic-resistant pathogens. It is, therefore, necessary to identify new types of drug leads that preferably work by a mechanism different from existing medicine.

Antimicrobial peptides (AMPs) are wide spread in nature and have been identified in the six kingdoms: bacteria, archaea, protists, fungi, plants, and animals. As an important element of innate immune systems, AMPs can fend off invading pathogens such as bacteria, viruses, fungi, and parasites [4–8]. Such a rapid response of AMPs to invaders is necessary considering the fast replication of bacteria in minutes and the slow response of our adaptive immune systems. Most of cationic AMPs can form an amphipathic structure for targeting anionic bacterial membranes. A large-scale membrane damage is difficult to repair, rendering it unlikely for pathogens to develop resistance to AMPs [4–6]. Indeed, resistance to tyrothricin has not been observed after decades of use [9]. The targeting of anionic bacterial membranes is usually facilitated by the positive charges of AMPs. This is consistent with the fact that 88% of the 2970 peptides registered in the Antimicrobial Peptide Database (APD; http://aps.unmc.edu/AP; visited April 2018) have a net charge, ranging from +1 to +30 at pH 7. Only 6% of AMPs in the current database are negatively charged [10].

Because the information in the APD was manually curated and well organized, it enabled us to search useful peptide templates more effectively. By screening representative members from the database, we identified multiple peptides that are potent against antibiotic-resistant pathogens. DASamP1 [11], a variant of temporin-PTa [12], is potent against methicillin-resistant *Staphylococcus aureus* (MRSA) USA300 both in vitro and in vivo. We also developed a database filtering technology to ab initio design anti-MRSA peptides [13]. Interestingly, the DFTamP1 peptide resembles temporins. These results suggest that temporins are likely useful candidates to combat MRSA that causes annual deaths comparable to HIV-1 [14]. Of note is that temporins can also have antiviral, antifungal, and antiparasitic effects as well [15–21]. To identify potentially useful peptide templates, this study investigated six natural peptides (four with unknown activity due to a limited amount of material and two with known antimicrobial activity as positive controls). These peptides were originally isolated from anuran skin secretions by Conlon and colleagues: temporins CPa and CPb from *Lithobates capito* (Tampa, Florida, USA), temporin-1Ga from *Rana grylio* (Nashville, TN, USA), temporin-1OLa from *Rana okaloosae* (Santa Rosa County, Florida, USA), temporin-1SPa from *Rana septentrionalis* (Somerset County, ME, USA), and temporin-1Oc from *Rana ornativentris* (Japan) [22–26]. Using synthetic peptides, we tested antibacterial, antifungal and anticancer activities of these peptides. Among them, temporin-1OLa was found to have a better cell selectivity index (i.e, high a-ntimicrobial activity but low cytotoxicity to human cells). We then further characterized this peptide mechanistically and determined its three-dimensional structure. The peptide possessed anti-biofilm activity and also protected animals from MRSA infection. Finally, we conducted bioinformatic analysis of all the temporins in the APD, leading to a classification of these peptides into six models and conferring significance to the structure of temporin-1OLa. Not only did this study enrich our existing knowledge on temporins but also shed new light on temporins by conducting the first structural bioinformatics study of this family of amphibian peptides. The new classification we proposed herein may facilitate future systematic decoding of the functional roles of temporins.

2. Materials and Methods

2.1. Peptide, Antibiotics and Chemicals

All peptides used in this study were chemically synthesized and purified to at least 95% by Genemed Synthesis Inc. (TX, USA). Fresh stocks of peptides were made by solubilizing them in autoclaved distilled water and their concentrations were determined by UV spectroscopy [27]. The sources of antibiotics are linezolid (Chem. Impex Intl. Inc, IL, USA), nafcillin (Chem. Impex Intl. Inc, IL, USA), vancomycin hydrochloride (Sigma Aldrich, MO, USA), rifamycin (Alfa Aesar, MA, USA) and daptomycin (BIOTANG Inc., MA, USA). Other chemicals were purchased from Sigma (MO, USA) unless specified.

2.2. Bacterial Strains and Growth Media

The bacterial strains used in this study to determine peptide activity included the Gram-positive strains *Staphylococcus aureus* USA300, USA200, USA400 LAC, Mu50, Newman, UAMS-1, *S. epidermidis* 1457, and *Bacillus subtilis* 168, as well as the Gram-negative isolates *Escherichia coli* ATCC 25922, *Klebsiella pneumoniae* ATCC 13883, and

Pseudomonas aeruginosa PAO1. All bacteria were cultivated using tryptic soy broth (TSB) (BD Bioscience MD, USA) unless stated otherwise.

2.3. Antibacterial Assays

The assay was performed using a lab protocol [13] adapted from the standard CLSI broth microdilution protocol [28] with some modifications. In brief, bacterial strains were inoculated overnight in TSB media. The overnight cultures were then freshly inoculated and allowed to grow to reach the exponential phase (OD_{600} ~0.5). The cultures were diluted accordingly to reach a bacterial count of 10^6 CFU/mL and 90 μL of this suspension was added to a 96 well microplate (Costar, Corning, NY) containing 10 μL of serially diluted peptide solutions and incubated overnight at 37°C for 20 h. The absorbance for bacterial growth was read with a CHROMATE microplate reader at 630 nm (GMI, Ramsey, MN). The wells not treated with antimicrobial compounds served as the bacterial control and the medium without bacteria inoculation was used as the negative control (blank). Additionally, peptide activity in the presence of various salts or serum and at different pH values were evaluated in the same way. The laboratory, where the work was conducted, has a BSL-2 permission to grow and use these bacteria for antimicrobial assays.

2.4. Synergistic Effects of Antimicrobial Peptides and Antibiotics

To understand the combined effects of temporin-1OLa and antibiotics, standard checkerboard's method was used. In brief, serial dilutions of 10 μL volume of 10× peptide dilutions made in 96 well microtiter plates, onto which another 10 μL of 10× antibiotics concentrations were added. The peptides were diluted horizontally from high to low concentrations, while the antibiotics were loaded vertically high to low concentrations. Finally, 80 μL of *S. aureus* USA300 (10^6 CFU/mL) in TSB medium was added on each well and the plates were included at 37°C for 20 h for MIC determination as described above. In this experiment, the synergistic effects between the peptides and antibiotics are expressed in terms of fractional inhibitory concentration as ΣFIC index. The ΣFICs were calculated as : $\Sigma FIC = FIC_{peptide} + FIC_{antibiotic}$, where $FIC_{peptide}$ is the MIC of peptide in the combination/MIC of peptide alone, and $FIC_{antibiotic}$ is the MIC of the antibiotic in the combination/MIC of antibiotic alone. The combination is considered synergistic when the ΣFIC is ≤ 0.5, additive when ΣFIC is >0.5 to ≥1, and indifferent when the ΣFIC is ≥ 2[2–9].

2.5. Antifungal Assays

Fungal strains included in the study were *Candida albicans* ATCC 10231, *C. glabrata* ATCC 2001 and *C. tropicalis* ATCC 13803. The fungi were grown in Remel Dex broth (Thermo Fisher Scientific, KS, USA). Antifungal assays were conducted essentially as described for antibacterial assays above, except for a higher starting density at an OD_{600} 0.02 and a longer incubation time of ~ 48 h prior to microplate reading.

2.6. Anticancer Assays

HeLa cells were maintained in DMEM high glucose media with 4 mM L-glutamine (NyClone) and 100 U/mL penicillin, 100 μg/mL streptomycin (pen/strep) (Life Technologies), and 10% (v/v) inactivated fetal bovine serum (FBS) (NyClone). Cells were

grown in 5% CO_2 at 37°C and detached from the culturing dish at 80% confluency using 0.025% trypsin-EDTA (NyClone) treatment. Effects of the peptide on cell viability were estimated by the MTS (3-(4,5-Dimethylthiazol-2-yl)-2,5-diphenyltetrazolium bromide) assay according to the manufacturer's protocol (Promega, USA) with minor modifications and as described [30]. Mouse breast cancer 4T1 cells were also cultivated for cytotoxicity evaluation of the peptides in a similar manner.

2.7. Killing Kinetics

These experiments were conducted similar to antibacterial assays described above with the following additions. Aliquots of cultures (10^5 CFU) treated with peptides were taken at 15, 30, 50, 90, and 120 min and plated on Luria-Bertani agar plates after 100-fold dilution. Colonies were counted after overnight incubation at 37°C.

2.8. Membrane Permeation by Fluorescence Spectroscopy

The experiment was performed as described [30]. In brief, 10 μL of serially diluted 10× peptide was mixed with 2 μL of propidium iodide (20 μM) and 88 μL of the *S. aureus* USA300 bacterial culture (final OD_{600} ~0.1 in TSB media) in 96-well corning COSTAR microtiter plates. The plates, with continuous shaking at 100 rpm at 37°C in a FLUOstar Omega microplate reader (BMG LABTECH Inc, NC, USA), were read every 5 minutes for a total duration of 3 h. The excitation and emission wavelengths for fluorescence measurement were set at 584 nm and 620 nm, respectively. Meanwhile, the bacterial growth was monitored at 600 nm. Plots were made with vendor's software using averaged values from duplicated experiments.

2.9. Electron Microscopy

For transmission electron microscopy (EM), *S. aureus* USA300 was grown in LB medium overnight at 37°C. Samples were made as previously described [13] and observed in an FEI Technai G2 TEM operated at 80 kV accelerating voltage at the University of Nebraska Medical Center (UNMC).

For scanning EM, *S. aureus* USA300 was treated with 6.2 μM peptide and fixed as above. Samples were washed with Sorensen's Buffer 3 changes, 5 min each change. Samples were postfixed in 1% osmium tetroxide in water for 30 min. After post-fixation, all samples were washed in Sorensen's buffer 3 changes at 5 min each change. All samples were dehydrated through a graded ethanol series (50%, 70%, 90%, 95%, 100% × 3 changes) for 10 min each dehydration step. Subsequently, samples were placed in HMDS 100% for 10 min for 3 changes and left in HMDS in open dishes in the fume hood overnight to allow the HMDS to evaporate. The following day the samples were mounted on 25 mm aluminum SEM stubs with carbon adhesive tabs. Silver paste was placed around the edges of the samples. Samples were Sputter Coated with 50 nm of gold/palladium in a Hummer VI Sputter Coater (Anatech Ltd.) and examined in a FEI Quanta 200 SEM operated at 25 Kv using the EM Core Facility on campus.

2.10. Antibiofilm Assay

Two types of static, plate mode experiments were conducted to assess the ability of the peptide in inhibiting biofilm formation (starting from 10^8 CFU/mL) as well as in disrupting 24-h preformed biofilms of *S. aureus* USA300 [31,32]. Quantification of the formed biomass or remaining biofilm was done using XTT (2,3-bis-(2-methoxy-4-nitro-5-sulfophenyl)-2H-tetrazolium-5-carboxanilide). To understand the effects of combination treatment the established biofilms were treated with either antibiotic alone or in combination with temporin-1OLa. The live bacteria in the plates were quantitated similarly using XTT.

2.11. Confocal Microscopy

S. aureus USA300 was grown to the exponential phase and diluted to 10^5 CFU/mL. Two mL of this bacterial culture was added to the chambers of cuvette (Borosilicate cover glass systems) and incubated for 24 h at 37°C for biofilm establishment. Media were then pipetted out from chambers and washed with normal saline to remove non-adhered bacteria. To see the effect of the peptide, 0.2 mL of 10× (125 μM) stocks was added followed by 1.8 mL TSB. Control cuvettes were treated with water. The cuvettes were again incubated for another 24 h. After washing, the remaining biofilms in chambers were stained with 10 μL of the LIVE/DEAD kit (Invitrogen Molecular Probes, USA) according to the manufacturer's instructions. The samples were examined on a confocal microscope (Zeiss 710) and the data were processed using the Zen 2010 software.

2.12. Hemolytic Assays

Human red blood cells (hRBC), obtained from the UNMC Blood Bank, were washed three times (800 g, 10 min each) with normal saline to remove plasma. A final of 0.5% or 2% hRBC solution was prepared in normal saline and used for the assay. 90 μL of this solution and 10 μL of serially diluted peptide solutions were incubated at 37°C for 1 h. The plate was then centrifuged at 1500 rpm for 5 min. Aliquots of the supernatant were transferred to a fresh 96 well microplate (Costar, Corning, NY) and absorbance was read at 545 nm to detect the amount of hemoglobin released. Percent lysis was calculated based on the extent of hemoglobin released (100% release in 1% Triton X-100 and 0% release in saline). In addition, peptide hemolysis was examined by incubating hRBCs solutions with and without bacteria.

2.13. Toxicity of Peptides on Human Keratinocytes

Peptides were assayed for potential in vitro toxicity using HaCaT keratinocytes. Briefly, cells were seeded at a density of 3×10^4 per well in a 96-well plate in DMEM supplemented with 10% fetal bovine serum (FBS), and incubated at 37°C in a 5% CO_2 atmosphere for 24 h. Wells were replaced with serum free media and treated with peptides at different concentrations for 1 h. After incubation, the cells were washed and incubated with 100 μL of DMEM media containing 20 μL of MTS for 2 h at 37°C. Absorbance were measured using the above ChroMate microplate reader.

2.14. HPLC Retention Time of Peptides

Peptide hydrophobicity was estimated by measuring its retention time on a Waters HPLC system equipped with an analytical reverse-phase Waters Symmetry300™ C18 column (5 μm; 150 × 4.6 mm). The peptide was eluted with a linear gradient of acetonitrile (containing 0.1% TFA) from 5% to 95% at a flow rate of 1 mL/min. The peptide peak was detected at 220 and 280 nm by UV.

2.15. NMR Spectroscopy

For NMR measurements, temporin-1OLa was solubilized in 0.3 ml of aqueous solution of 90% H_2O and 10% D_2O containing SDS at pH 5.6. The peptide/SDS molar ratio was 1:60. The pH of each sample was adjusted and measured directly in the 5-mm NMR tube with a micro-pH electrode (Wilmad-Labglass). As described previously [33], all proton NMR data (NOESY, TOCSY and DQF-COSY) [34] were collected using a spectral width of 6,000 Hz in both dimensions at 35°C on a Bruker 600 MHz NMR spectrometer equipped with a triple-resonance cryoprobe. The water signal was suppressed by low power presaturation during both the relaxation delay and the mixing period in NOESY experiments and during relaxation delay only for TOCSY and DQF-COSY experiments. To obtain backbone ^{15}N, $^{13}C\alpha$, and $^{13}C\beta$ chemical shifts, natural abundance HSQC spectra were collected. All NMR data were processed on an Octane workstation using the NMRPipe software [35]. NMR data were apodized by a 63° shifted squared sine-bell window function in both dimensions, zero-filled prior to Fourier transformation to yield a data matrix of 2,048 × 1,024. NMR data were analyzed with PIPP [36]. The peptide proton signals were assigned using the standard procedure [34] and validated using ^{15}N and ^{13}C chemical shifts of the peptides.

2.16. Structure Calculation

The three-dimensional structures of temporin-1OLa were calculated based on both distance and angle restraints by using the NIH-Xplor program [37]. The distance restraints were obtained by classifying the NOE cross peak volumes into strong (1.8–2.8 Å), medium (1.8–3.8 Å), weak (1.8–5.0 Å), and very weak (1.8–6.0 Å) ranges. Peptide backbone restraints were predicted based on backbone $^{1}H\alpha$, $^{13}C\alpha$, $^{13}C\beta$, and ^{15}N chemical shifts [38]. In total, 200 structures were calculated. An ensemble of 20 structures with the lowest total energy was chosen. This final ensemble of the accepted structures satisfies the following criteria: no distance violations greater than 0.30 Å, rmsd for bond deviations from the ideal less than 0.01 Å, and rmsd for angle deviations from the ideal less than 5°.

2.17. Bioinformatics of Temporins

Bioinformatic analysis was conducted using the APD and associated tools (http://aps.unmc.edu/AP). The first version of the APD [39] was established in 2003 and the updated versions were published in 2009 and 2016, respectively [10,40]. First, short peptides (13–14 residues) with known amino acid sequence but unknown biological activity were searched using “DXWZ” in the Name field and six natural peptides were selected for this study (Table 1). Second, peptide molecular weight, net charge, hydrophobic content, amino acid contents and Boman index were calculated using the prediction interface. Third, temporins registered in the APD were searched and analyzed to identify the sequence

patterns based on the distribution of proline residues (see the text). Although our analysis is limited to antimicrobial activity here, the relationship of this classification with other biological functions (e.g., anti-diabetic) of temporins remains to be established [41]. The use of the APD is not limited to the above analyses. For example, database search using "synerg" in the "Additional Info" field also reveals synergistic interactions between temporins such as temporins A and L [42,43].

2.18. In Vivo Assays

The potency of temporin-1OLa was tested *in vivo* using wax moths *Galleria mellonella* (distributed by Timerline Live Pet Foods Marion, IL) as described [44]. Survival rates were plotted as a function of time using Graphpad prism software (CA, USA).

2.19. Statistics

All experiments were replicated at least twice. For hemolysis, biofilm, cell viability and bactericidal enumeration experiments, plots represent the average values with standard deviation error bars. For membrane permeation experiments, data points from duplicated wells were processed using the vendor's software (MARS, BMG Lab tech). For all experiments, the level of significance was determined by performing paired Student t-test with parameters of two tailed distribution and p values > 0.05 were considered significant (*).

3. Results

3.1. Antimicrobial and Anticancer Activities of Six Temporins

The amino acid sequences and some properties of the six temporins studied here are listed in Table 1 and the peptide quality data are provided as supporting information (Fig. S1). To map the antibacterial activity spectrum of the six temproins, both Gram-positive and Gram-negative bacteria were used. Similar to vancomycin, these peptides were active against Gram-positive methicillin-resistant *Staphylococcus aureus* USA300*, Staphylococcus epidermidis* 1457, *Bacillus subtilis* 168, but not Gram-negative *Escherichia coli* ATCC 25922, *Pseudomonas aeruginosa* PAO1, and *Klebsiella pneumoniae* ATCC 13883, indicating a preference for Gram-positive pathogens (Table 2). Interestingly, temporin-CPa showed moderate activity against *E. coli* and *S. epidermidis* (minimal inhibitory concentration MIC = 12.5 μM) but not against *S. aureus* till 25 μM. The lack of anti-*S. aureus* activity of temporin-CPa might be due to its low hydrophobic content (53%, see Table 1). Except for temporin-CPa, these peptides were also active against multiple *S. aureus* clinical strains (Table S1, Supporting information).

To identify the candidate with therapeutic potential, we then compared the cytotoxicity of the six peptides based on the 50% hemolytic concentration (HL_{50}) of human red blood cells (hRBCs). While temporin-1Oc was highly active against *S. aureus* USA300 (MIC 1.56 μM), it was also most toxic (HL_{50}< 12.5 μM in Table 2). The next more hemolytic peptide was temporin-1Ga with an HL_{50} of 12.5 μM. As the MIC of this peptide against *S. aureus* USA300 was 3.1 μM, this led to a cell selectivity index CSI (= HL_{50}/MIC) of 12.5/3.1 = 4. Although temporin-CPa and temporin-CPb showed high HL_{50} > 100 μM, they were either

moderately or poorly active against *S. aureus* USA300 (MIC 12.5 or >25 μM). Temporin-1OLa appeared to be more cell selective. It displayed an MIC of 1.6–3.1 μM against MRSA and HL_{50} of 50 μM, leading to a CSI of 16–32. This is similar to the index we previously obtained for temporin-PTa, another amphibian peptide [13]. To further understand the cytotoxicity of these peptides to human erythrocytes, we measured the retention times of these peptides on a reverse-phase HPLC column. A short retention time indicates lower hydrophobicity. Temporins-CPa and CPb have the shortest retention times, corresponding to their poorest hemolysis (Table 2). In contrast, those more hemolytic peptides showed longer HPLC retention times. Overall, peptide hemolytic ability correlated well with peptide hydrophobicity estimated from HPLC.

To further define the peptide activity spectrum, we also tested antifungal and anticancer activity of these six peptides and the results are summarized in Table 3. Temporin-1Ga and temporin-1OLa were found to be more active against yeast *C. albicans*, *C. glabrata*, and *C. tropicalis*. Interestingly, temporin-1Ga was more toxic to mouse breast cancer cells 4T1 (LC_{50} = 20 μM), while temporin-1OLa showed higher toxicity to Hela cells (LC_{50} = 25 μM). For comparison, we also evaluated the cytotoxicity of these peptides to human skin HaCaT cells. The 50% lethal concentration (LC_{50}) was 100 μM for temporin-1OLa and 40 μM for temporin-1Ga, respectively. The higher cytotoxicity of temporin-1Ga agrees with its high hydrophobicity (Table 2). This led to an anticancer cell selectivity of 2 for temporin-1Ga and 4 for temporin-1OLa. Such CSI values (2–4) are rather low. Using the same LC_{50} for HaCaT cells, the CSI would be 32–64 for temporin-1OLa against *S. aureus* USA300 (MIC 1.6–3.1 μM). Therefore, temporin-1OLa has a much higher CSI as an antibacterial agent than as anticancer agent.

Since bacteria usually exist during infection treatment, we also evaluated the presence of *S. aureus* USA300 on hemolysis. At different bacterial CFUs, we found similar hemolysis at peptide concentrations of 12.5, 25, and 100 μM. However, the decrease in peptide hemolysis was more pronounced at 50 μM of temporin-1OLa at 2% RBCs (Fig. 1A). It has been documented that peptide HL_{50} concentrations depend on cell densities of RBCs [30,45]. Consequently, we also tested this effect at a reduced number of RBCs. When 0.5% RBCs were used in the assay, we observed a similar outcome (Fig. S2), indicative of an effect irrespective of the two concentrations of hRBCs. We also asked whether this enhanced selectivity of the peptide originated from direct antibacterial activity of the peptide. To test this, we utilized *E. coli* ATCC 25922, which was not inhibited by temporin-1OLa at 50 μM (Table 2). Again, we observed a reduced hemolytic ability of the peptide primarily at 50 μM of temporin-1OLa, which happens to correspond to HL_{50} of the peptide (Fig. S2 supporting info). Thus, this enhanced cell selectivity at HL_{50} of the peptide is not due to direct bacterial killing. More likely, the cationic peptide was able to partition between eukaryotic and prokaryotic cells and the negative charge on bacterial surface could be important for preferred electrostatic interactions, thereby reducing the amount of peptide available for hemolysis.

3.2. Mechanism of Action of Temporin-1OLa

The higher cell selectivity made temporin-1OLa an interesting candidate for further characterization. We then studied the effects of salts, pH and human serum on the antibacterial activity of this temporin. The MIC was 3.1 μM between pH 7–8 and increased to 6.2 μM at pH 6.8 (Table 4). Furthermore, there was no change in the peptide MIC in the presence of 150 mM NaCl. However, serum did influence peptide MIC. In the presence of 10% human serum during the entire assay, the MIC was increased eight-fold from 3.1 to 25 μM, implying its binding to serum proteins.

Next, we compared bacterial killing ability of these peptides based on colony counting. After 30 min incubation with 3.1 μM peptide, *S. aureus* USA300 was essentially eliminated by peptides temporins-1Ga, 1OLa, and 1Oc, while temporins-CPa and CPb did not work (Fig. 2A). After 90 min incubation, temporin-CPb was able to kill ~50% *S. aureus* USA300, while temporin-CPa remained ineffective. Temporin-1SPa was also effective with less than 50% bacterial survival after 90 min. We also compared in detail the killing efficiency of temporin-1OLa and temporin-1SPa. Temporin-1OLa killed *S. aureus* rapidly in 30 min. In contrast, temporin-1SPa is unable to at this concentration after 120 min (Fig. 2B). Overall, such a killing efficiency is consistent with MIC values with temporin-1Ga, temporin-1OLa and temporin-1Oc more active (MIC 1.56–3.1 μM) against *S. aureus* USA300, whereas temporin-CPa was inactive till 25 μM (Table 2). The rapid staphylococcal killing of temporin-1OLa suggests that it acted on bacterial membranes (Fig. 2).

To validate membrane targeting of temporin-1OLa, we then followed bacterial absorbance and fluorescence changes of propidium iodide after peptide treatment (Fig. 3). Previous studies indicate that only membrane-active AMPs such as daptomycin and human cathelicidin derived 17BIPHE2 can permeate bacterial membranes, but not non-membrane targeting antibiotics vancomycin or rifamycin [30]. Membrane damage by the antibiotic opens the door to to the entrance of a membrane non-permeable DNA-binding dye, propidium iodide (molecular mass 668.4), into bacterial cells and association with DNA, leading to 20–30 fold increase in fluorescence. As shown in Fig. 3B, we observed little increase in fluorescence in the absence of the peptide or when treated with low concentrations of the peptide (1.56 μM or less). However, there is a clear increase in fluorescence when the peptide concentration reached 3.1 μM or higher. These results indicate that the peptide interacted with bacterial membranes to exert its antibacterial activity. To connect the bacterial killing (membrane permeation) with inhibition, we conducted the fluorescence experiment simultaneously with the bacterial growth inhibition experiment. At 0.78 or 1.56 μM, *S. aureus* USA300 grew well similar to the untreated control. However, bacterial growth was entirely inhibited once the concentration of temporin-1OLa reached 3.1 μM (Fig. 3A). Therefore, the growth inhibition of *S. aureus* by the peptide at 3.1 μM resulted from membrane damage-caused cell death.

To directly view the damaged bacteria, we also recorded the transmission electron microscopy of *S. aureus* USA300. In the untreated control, the cell of *S. aureus* USA300 had a rounded shape consistent with its coccal character. In the presented negative stained transmission electron micrographic image, clear opacity could be seen around the cell surface (Fig. 4A). After the peptide treatment, however, damaged cells were observed and

some became transparent (Fig. 4B), indicative of cell leakage. In addition, an adjacent deformed ghost cell was an outcome of the loss of membrane rigidity. To further confirm the damaging effect of this peptide, we also observed *S. aureus* USA300 treated at 6.2 μM peptide using scanning electron microscopy. At a lower treatment concentration, we saw both undamaged (similar to those untreated in Fig. 4C) and damaged cells (Fig. 4D). These results further support membranolytic property of temporin-1OLa.

3.3. Anti-biofilm Ability of Temporin-1OLa

In nature, bacteria are rarely living in the planktonic state as we cultivated in laboratories. More often they form biofilms to house the community. The “house” is usually surface-anchored and decorated with layers of biopolymers such as DNA, proteins and polysaccharides, making it more challenging to treat medically [46]. It is said that a thousand fold of traditional antibiotics could be required to treat biofilms [47]. We then evaluated the antibiofilm effects of temporin-1OLa on biofilms. The first experiment tested the biofilm inhibition of temporin-1OLa, which showed a concentration-dependent inhibition of biofilm formation of *S. aureus* USA300 (Fig. 5A). Because of a high starting CFU (1×10^8), biofilm formation was inhibited at 6.2 μM and nearly completely inhibited at 12.5 μM (i.e., fourfold MIC). The second experiment tested the ability of the peptide to disrupt preformed biofilms. A similar dose-dependent anti-biofilm effect was visible (Fig. 5B). After treatment with 6.25–12.5 μM of the peptide for 24 h, only ~20% *S. aureus* biofilms remained. The bacterial killing in the biofilms was directly observed by confocal microscopy. We observed live cells (green in Fig. 6A) without peptide treatment. However, a large population of the cells was dead (red) after peptide treatment (Fig. 6B). These experiments underscore that temporin-1OLa was able to inhibit the biofilm formation and kill *S. aureus* in biofilms.

To further remove preformed biofilms, we also studied the effect of combined treatment, which appears to be especially important to remove preformed biofilms [48]. Several antibiotics were tested in combination with temporin-1OLa. Only linezolid showed an additive effect with the peptide (fractional inhibitory concentration, FIC = 0.624 in Table S2, supporting info). Such an additive effect might result from a different mechanism of action of linezolid, which stops protein synthesis, while temporin-1OLa targets bacterial membranes. The antibiotic linezolid is currently used to treat serious infections caused by Gram-positive bacteria. We then evaluated the biofilm disruption ability of the peptide with linezolid. Indeed, the combination could reduce biofilms more effectively (Fig. 5D) than those treated with antibiotic alone (Fig. 5C).

3.4. In vivo Efficacy of Temporin-1OLa

To further evaluate the therapeutic potential of temporin-1OLa, we also tested its in vivo efficacy in an established invertebrate model *Galleria mellonella* [44]. In the absence of the peptide or in the presence of a low level of peptide (8 mg/kg), an inoculation of *S. aureus* USA300 at 1×10^6 CFU per insect led to the death of animals in 2–3 days (Fig. 7, red and green curves), whereas very few animals died in the saline treated group, implying bacterial infection was responsible for the death of wax moths. However, the deaths of animals were reduced when treated with a single dose of temporin-1OLa at 32 mg/kg 2 h ahead of

bacterial infection (Fig. 7, purple lines). Therefore, temporin-1OLa also has the ability to protect the wax moths from staphylococcal infection (Fig. 7). This protection effect is similar to merecidin, a peptide antimicrobial designed based on the only human cathelicidin LL-37 [30,49].

3.5. 3D Structure of Temporin-1OLa

Since our results above indicate that temporin-1OLa targets bacterial membranes (Fig. 3), we determined its three-dimensional structure bound to membrane-mimetic micelles of deuterated SDS [33,50]. The peptide/SDS molar ratio was set to 1:60 so that one peptide was associated with one micelle. We utilized the improved 2D NMR method for structural determination [50]. Different from the traditional 2D NMR method that involves protons only [34], the improved 2D NMR method also records natural abundance ^{15}N and ^{13}C heteronuclear correlated spectra to validate the proton assignments and refine the 3D structure [14]. The chemical shifts of temporin-1OLa are provided in Table S3 (supporting information). Based on the Hα chemical shifts, we calculated secondary shifts for temporin-1OLa relative to the random coil values measured by Wüthrich [34]. Residues P3-I12 possessed negative secondary shifts, suggesting a helical region (Figure S3, supporting information). For structure determination of the peptide, we obtained 137 NMR restraints (20 backbone angles and 117 distances). Ramachandran plot analysis of 20 structures with the lowest energies revealed 91.1% of the peptide backbone angles were located in the most favored region and 8.9% in the additional allowed region, indicating high quality. Structural analysis [51] indicates that residues 3–12 of temporin-1OLa are α-helical (Fig. 8A). The rmsd for superimposing the backbone atoms for the helical region of the 20 structures was 0.51 Å. Because hydrophilic (e.g., K6 and K11) and hydrophobic side chains (e.g., F4, L5, I8, L9, and I12) of the peptide are located on opposite sides, the membrane-bound structure of temporin-1OLa is an amphipathic helix (Fig. 8B). Of particular interest is that the aromatic ring of F1 packs with the sidechain of L2 at the N-terminus and is adjacent to the aromatic ring of F4, thereby extending the hydrophobic surface. The importance of phenylalanines in membrane anchoring has been illustrated in multiple examples, including a bacterial membrane anchor, antimicrobial and anticancer peptide aurein 1.2, and human cathelicidin LL-37 peptides [50,52]. Temporin-1OLa is dominated by hydrophobic amino acids with only two lysines K6 and K11 (see potential surface in Fig. 8C & D). Such a structure shines light on the activity spectrum of temporin-1OLa (Table 2).

3.6. Bioinformatic Insight into Temporins

With the increase in the number of temporins identified in nature, it is useful to conduct a bioinformatic analysis to gain insight into the general design principles of natural temporins. For this purpose, we utilized the antimicrobial peptide database [39]. At the time of this analysis, there were 121 temporins [10]. These temporins were 8–17 amino acid long (average 13.67) with a net charge between 0-+4 (average +1.02) and hydrophobic content in the range of 46–76% (average 63.06%). The averaged amino acid use of temporins is plotted in Fig. 9A. It is evident that the dominant hydrophobic amino acids in temporins were leucine (29.86%), phenylalanine (11.72%), and isoleucine (10.7%). Other commonly used amino acids included glycine, proline, and serine. In terms of basic amino acids, temporins usually use lysine (6.97%) as the percentages for both arginine (1.14%) and histidine (0.9%)

were very low. There was no cysteine in temporins (no disulfide bonds) and amino acids such as methionine, tryptophan, tyrosine, glutamine, glutamate and aspartate were very low. Alternatively, the amino acid use in temporins could also be estimated based on the peptide counts containing a particular amino acid (Fig. 9B). Interestingly, this amino acid occurrence in temporins remarkably resembles the amino acid content on average. A clear deviation is leucine since its percentage is high (30%) due to its presence of multiple times in the same sequence. Thus, the amino acid use (i.e. signature) in temporins is biased toward hydrophobic ones.

4. Discussion

AMPs have been discovered in both invertebrates and vertebrates. According to the APD, 35% of the natural peptides originated from amphibians [10]. One important reason for this is the wide distribution of frogs on all the continents. In the APD, there are 308 amphibian AMPs from America, 88 from Africa, 487 from Asia, 93 from Australia, and 59 from Europe. Due to limited amounts of materials, however, the biological activity of a small population (6%) of these peptides in the APD (collected earlier for the sake of completeness) is not defined. This study established four anuran peptides as AMPs originally discovered by Conlon and colleagues [22–26]. As a positive control, it is interesting to note that our activity data (Tables 2–3) for temporin-CPa are comparable to those found previously by Conlon and colleagues (*E. coli,* MIC 25 μM; *C. albicans,* MIC 25 μM; *S. aureus*, MIC 50 μM) [22]. In addition, the MIC (2 μM) of temporin-1Oc against *S. aureus* found previously [26] is also similar to that in Table 2. These similarities validated the activity data we obtained in this study. For temporin-1SPa, we found activity against Gram-positive bacteria but not Gram-negative bacteria (Table 2) similar to a similar peptide temporin-1SPb found previously [25]. Different from temporin-1SPb, however, temporin-1SPa was found here to be antifungal. Interestingly, temporin-1Ga in Table 2 is more active against *S. aureus* than temporin-1Gb [23]. Through our study, temporin-1OLa is identified as a more promising candidate for future development because of its higher cell selectivity (Table 2). Such preference of bacterial targeting is usually attributed to the differences in membranes: rich in anionic lipids in bacteria but zwitterionic lipids in mammalian cells [4–7, 53, 54]. In the presence of bacteria, the peptide hemolytic concentration was reduced mainly at the 50% hemolysis concentration (Fig. 1).

Unlike magainins with a broad activity spectrum [55], temporins are mainly active against Gram-positive pathogens [54]. Sequence analysis of these six peptides revealed relatively high hydrophobic contents, ranging from 57–69% with a net charge of 2–3 (Table 1). Likewise, the amino acid signature of all the temporins in the APD indicates that leucine is rather abundant (~30% in Fig. 9). Remarkably, both isoleucine and phenylalanine also satisfied the definition of “frequently occurring amino acids”, which we defined previously based on such sequence signatures from a variety of peptide groups [7,10]. Glycine is another abundant amino acid. On the right side of Fig. 1A, serine and lysine showed higher contents than other amino acids. It appears that such an amino acid feature determines peptide activity spectrum [30]. This is consistent with our previous finding that a change of a hydrophilic amino acid into proline, or vice versa, influences the peptide activity spectrum. However, the activity against *E. coli* was 8–16 fold less than that against *S. aureus* [13].

Therefore, a single amino acid change in temporins (Fig. 8) did not alter its dominant activity against Gram-positive pathogens.

Because proline appears to be an important structure and activity modulator, we can classify temporins into six models based on the position and number of prolines in the sequences (Table 5). The first model does not contain any proline in the sequence. There are 31 such sequences in the current APD (Table 5). Model 2, with a proline at the N-terminus (usually at position 3), appears to be most common. We found 75 such sequences. The third model contains two proline amino acids at the N-terminus. We found four such peptides where the prolines can be adjacent or separated by up to three residues. The fourth model consists of a proline residue at the C-terminus (Table 5). Currently, temporin-PTa is the only example. The fifth model contains two proline residues at the C-terminus of the sequence. Temporin-LTc is such an example. Finally, the sixth model is characterized by the presence of proline at both peptide ends. There are nine such sequences in the APD (Table 5). As summarized in Table 5, model 2 is the major sequence pattern for temporins (62%) in the current database. These temporins share a similar sequence pattern (LL**P**LLXXLLXXLL), where L represents a general hydrophobic amino acid (e.g., F, L, and I) while underlined X's are usually G, S, N, Q, T, K, R, and H. Wade previously identified a consensus sequence FLPLIASLLSKLL for temporins [56], or model-2 temporins in our classification. Mangoni and Conlon also observed conserved sequence patterns for temporins [24,54]. Based on our classification, we also attempted to identify the correlation between peptide parameters for a better understanding of antimicrobial and cytotoxic effects (Table S4 supporting information). Using all the temporins collected, we did not see good correlations and the correlations did not improve when using model 2 peptides alone, indicating a more complex relationship yet to be elucidated. Indeed, previous studies revealed that the activity of temporins and their analogs are related to multiple factors, including amino acid composition, sequence, chirality, helicity, and positive charge [56]. Likewise, such a single-parameter correlation was not observed for a series of aurein 1.2 peptides, either [50]. However, it seems that less antimicrobial and hemolytic temporins are usually less hydrophobic (bold in Table S3). In addition, it is noticed that temporins with a net charge of +1 or less or with a shorter sequences (e.g., 10 amino acids) are usually inactive [54].

The formation of an amphipathic helix and its membrane permeation is proposed to be important for antimicrobial activity of temporins [21,24,54,57]. Because proline is an important structure and activity modulator, our proline-based classification of temporins into six models here may facilitate a more complete understanding of the functional roles of temporins, including the recently discovered anti-diabetic role [41]. Interestingly, temporin-1OLa belongs to model 2, the major sequence pattern of temporins. We propose that the 3D structure of this temporin (Fig. 7) may be useful to understand the activity of similar peptides. In the structure of temporin-1OLa, P3 serves as a helix-starting signal. A pair of hydrophobic amino acids F1 and L2 in front of P3 extends the hydrophobic surface, likely enhancing peptide activity. It is noted that the N-terminal structure of temporin-1OLa is frayed (Fig. 7A). Interestingly, a structurally frayed N-terminus was also observed in temporin-SHb, another model 2 peptide. Two model 1 peptides, temporin-SHa and temporin-SHc [58], also displayed frayed N-terminal ends. DFTamP1, the first peptide

designed based on the database filtering technology, shares this temporin feature since its N-terminal residues are more mobile as well [13]. It appears that a more mobile N-terminus is a general feature for temporins. However, the participation of the N-terminal hydrophobic amino acids in peptide action is anticipated. An N-terminal hydrophobic patch in front of a helical domain also occurs in biologically active peptides discovered in the venoms of spiders and scorpions (reviewed in ref [59]). Therefore, such a molecular design (i.e., hydrophobic patch + short two-turn helix) may be of general importance for host innate defense and perhaps the predation of spiders and scorpions on other animals.

5. Conclusion

This study established temporins CPb, 1Ga, 1OLa and 1SPa as antimicrobial peptides with activity mainly against Gram-positive bacteria (Table 2). Temporins 1Ga and 1OLa also showed antifungal and anticancer effects as well (Table 3). NMR structural studies reveal a hydrophobic patch followed by a classic amphipathic structure (Fig. 8B), which may explain the antimicrobial efficacy of this peptide in vitro and in vivo (Fig. 7). Importantly, temporin-1OLa, a model 2 peptide with a proline at position 3, shares a sequence pattern with 62% temporins in the antimicrobial peptide database, making it a potentially useful model to understand other peptides in the same class. Our proline-based classification of temporins into six models can be useful for a more complete understanding of the functional roles of these innate immune peptides.

Supplementary Material

Refer to Web version on PubMed Central for supplementary material.

Acknowledgments

This study was supported by Nebraska Research Initiative (NRI) and Nebraska LB905 through the Pediatric Cancer Research Group and in part by the NIAID/NIH grant R01 AI105147 to GW. XW and YZ were also supported by the China Scholarship Council. We also thank Tom Bargar, Nicholas Conoan, Janice A. Taylor and James R. Talaskafor technical assistance.

Abbreviations

AMPs	antimicrobial peptides
APD	antimicrobial peptide database
CFU	colony forming units
CSI	cell selectivity index
EM	Electron microscopy
HIV-1	human immunodeficiency virus type 1
HL_{50}	the peptide concentration that causes 50% hemolysis
HPLC	high pressure liquid chromatography

hRBC	human red blood cell
MIC	minimal inhibitory concentration
MRSA	methicillin-resistant *Staphylococcus aureus*
NMR	nuclear magnetic resonance
SDS	sodium dodecylsulfate
TSB	tryptic soy broth

References

1. Nobel lecturehttp://www.nobelprize.org/nobel_prizes/medicine/laureates/1945/fleming-lecture.pdf
2. Eliopoulos GM, Willey S, Reiszner E, Spitzer PG, Caputo G, Moellering RC Jr. In vitro and in vivo activity of LY 146032, a new cyclic lipopeptide antibiotic. Antimicrob Agents Chemother. 1986; 30:532–535. [PubMed: 3024560]
3. Nobel lecturehttps://www.nobelprize.org/nobel_prizes/medicine/laureates/2015/tu-lecture.html
4. Zasloff M. Antimicrobial peptides of multicellular organisms. Nature. 2002; 415:389–395. [PubMed: 11807545]
5. Hancock RE, Sahl HG. Antimicrobial and host-defense peptides as new anti-infective therapeutic strategies. Nat Biotechnol. 2006; 24:1551–1557. [PubMed: 17160061]
6. Mishra B, Reiling S, Zarena D, Wang G. Host defense antimicrobial peptide as antibiotics: design and application strategies. Curr Opin Chem Biol. 2017; 38:87–96. [PubMed: 28399505]
7. WangG, editorAntimicrobial Peptides: Discovery, Design and Novel Therapeutic Strategies2. CABI; England: 2017
8. Merrifield RB, Juvvadi P, Andreu D, Ubach J, Boman A, Boman HG. Retro and retroenantio analogs of cecropin-melittin hybrids. Proc Natl Acad Sci USA. 1995; 92:3449–3453. [PubMed: 7724582]
9. Strauss-Grabo M, Atiyem S, Le T, Kretschmar M. Decade-long use of the antimicrobial peptide combination tyrothricin does not pose a major risk of acquired resistance with gram-positive bacteria and Candida spp. Pharmazie. 2014; 69:838–841. [PubMed: 25985581]
10. Wang G, Li X, Wang Z. APD3: the antimicrobial peptide database as a tool for research and education. Nucleic Acids Res. 2016; 44:D1087–D1093. [PubMed: 26602694]
11. Menousek J, Mishra B, Hanke ML, Heim CE, Kielian T, Wang G. Database screening and in vivo efficacy of antimicrobial peptides against methicillin-resistant Staphylococcus aureus USA300. Int J Antimicrob Agents. 2012; 39:402–406. [PubMed: 22445495]
12. Conlon JM, Kolodziejek J, Nowotny N, Leprince J, Vaudry H, Coquet L, Jouenne T, King JD. Characterization of antimicrobial peptides from the skin secretions of the Malaysian frogs, *Odorrana hosii*and *Hylarana picturata*(Anura:Ranidae). Toxicon. 2008; 52:465–473. [PubMed: 18621071]
13. Mishra B, Wang G. *Ab initio* design of potent anti-MRSA peptides based on database filtering technology. J Am Chem Soc. 2012; 134:12426–12429. [PubMed: 22803960]
14. Wang G. Database-guided discovery of potent peptides to combat HIV-1 or Superbugs. Pharmaceuticals. 2013; 6:728–758. [PubMed: 24276259]
15. Marcocci ME, Amatore D, Villa S, Casciaro B, Aimola P, Franci G, Grieco P, Galdiero M, Palamara AT, Mangoni ML, Nencioni L. The Amphibian Antimicrobial Peptide Temporin B Inhibits *In Vitro* Herpes Simplex Virus 1 Infection. Antimicrob Agents Chemother. 2018; 62 pii: e02367–17.
16. Wang G, Waston K, Peterkofsky A, Buckheit R Jr. Identification of novel human immunodeficiency virus type 1-inhibitory peptides based on the antimicrobial peptide database. Antimicrob Agents Chemother. 2010; 54:1343–1346. [PubMed: 20086159]

17. Chinchar VG, Bryan L, Silphadaung U, Noga E, Wade D, Rollins-Smith L. Inactivation of viruses infecting ectothermic animals by amphibian and piscine antimicrobial peptides. Virology. 2004; 323:268–275. [PubMed: 15193922]

18. Conlon JM, Kolodziejek J, Nowotny N. Antimicrobial peptides from ranid frogs: taxonomic and phylogenetic markers and a potential source of new therapeutic agents. Biochim Biophys Acta. 2004; 1696:1–14. [PubMed: 14726199]

19. Rollins-Smith LA, Carey C, Longcore J, Doersam JK, Boutte A, Bruzgal JE, Conlon JM. Activity of antimicrobial skin peptides from ranid frogs against Batrachochytrium dendrobatidis, the chytrid fungus associated with global amphibian declines. Dev Comp Immunol. 2002; 26:471–479. [PubMed: 11906726]

20. Mangoni ML, Saugar JM, Dellisanti M, Barra D, Simmaco M, Rivas L. Temporins, small antimicrobial peptides with leishmanicidal activity. J Biol Chem. 2005; 280:984–990. [PubMed: 15513914]

21. Raja Z, André S, Abbassi F, Humblot V, Lequin O, Bouceba T, Correia I, Casale S, Foulon T, Sereno D, Oury B, Ladram A. Insight into the mechanism of action of temporin-SHa, a new broad-spectrum antiparasitic and antibacterial agent. PLoS One. 2017; 12:e0174024. [PubMed: 28319176]

22. Conlon JM, Meetani MA, Coquet L, Jouenne T, Leprince J, Vaudry H, Kolodziejek J, Nowotny N, King JD. Antimicrobial peptides from the skin secretions of the New World frogs *Lithobates capito*and *Lithobates warszewitschii*(Ranidae). Peptides. 2009; 30:1775–1781. [PubMed: 19635516]

23. Kim JB, Halverson T, Basir YJ, Dulka J, Knoop FC, Abel PW, Conlon JM. Purification and characterization of antimicrobial and vasorelaxant peptides from skin extracts and skin secretions of the North American pig frog *Rana grylio*. Regul Pept. 2000; 90:53–60. [PubMed: 10828493]

24. Conlon JM, Coquet L, Leprince J, Jouenne T, Vaudry H, Kolodziejek J, Nowotny N, Bevier CR, Moler PE. Peptidomic analysis of skin secretions from *Rana heckscheri* and *Rana okaloosae* provides insight into phylogenetic relationships among frogs of the Aquarana species group. Regul Pept. 2007; 138:87–93. [PubMed: 17005262]

25. Bevier CR, Sonnevend A, Kolodziejek J, Nowotny N, Nielsen PF, Conlon JM. Purification and characterization of antimicrobial peptides from the skin secretions of the mink frog (Rana septentrionalis). Comp Biochem Physiol C Toxicol Pharmacol. 2004; 139:31–38. [PubMed: 15556063]

26. Kim JB, Iwamuro S, Knoop FC, Conlon JM. Antimicrobial peptides from the skin of the Japanese mountain brown frog, Rana ornativentris. J Peptide Res. 2001; 58:349–356. [PubMed: 11892844]

27. Waddell WJ. A simple ultraviolet spectrophotometric method for the determination of protein. J Lab Clin Med. 1956; 48:311–314. [PubMed: 13346201]

28. Clinical and Laboratory Standards Institute, M27-A3Reference method for broth dilution antifungal susceptibility testing of yeasts; Approved standard3. 2008

29. Hu ZQ, Zhao WH, Yoda Y, Asano N, Hara Y, Shimamura T. Additive, indifferent and antagonistic effects in combinations of epigallocatechin gallate with 12 non-beta-lactam antibiotics against methicillin-resistant *Staphylococcus aureus*. J Antimicrob Chemother. 2002; 50:1051–1054. [PubMed: 12461032]

30. Wang X, Mishra B, Lushinikova T, Narayana JL, Wang G. Amino acid composition determines peptide activity spectrum and hot spot-based design of merecidin. Adv Biosys. 2018; 2:1700259.

31. Dean SN, Bishop BM, van Hoek ML. Natural and synthetic cathelicidin peptides with anti-microbial and anti-biofilm activity against *Staphylococcus aureus*. BMC Microbiol. 2011; 11:114. [PubMed: 21605457]

32. Mishra B, Lushnikova T, Golla RM, Wang X, Wang G. Design and surface immobilization of short anti-biofilm peptides. Acta Biomater. 2017; 49:316–328. [PubMed: 27915018]

33. Zarena D, Mishra B, Lushnikova T, Wang F, Wang G. The π Configuration of the WWW Motif of a Short Trp-Rich Peptide Is Critical for Targeting Bacterial Membranes, Disrupting Preformed Biofilms, and Killing Methicillin-Resistant *Staphylococcus aureus*. Biochemistry. 2017; 56:4039–4043. [PubMed: 28731688]

34. WüthrichK. NMR of Proteins and Nucleic AcidsWiley; New York: 1986

35. Delaglio F, Grzesiek S, Vuister GW, Zhu G, Pfeifer J, Bax A. NMRPipe: a multidimensional spectral processing system based on UNIX pipes. J Biomol NMR. 1995; 6:277–293. [PubMed: 8520220]
36. Garrett DS, Powers R, Gronenborn AM, Clore GM. A common sense approach to peak picking two-, three- and four-dimensional spectra using automatic computer analysis of contour diagrams. J Magn Reson. 1991; 95:214–220.
37. Schwieters CD, Kuszewski J, Tjandra N, Clore GM. The Xplor-NIH NMR molecular structure determination package. J Magn Reson. 2003; 160:65–73. [PubMed: 12565051]
38. Cornilescu G, Delaglio F, Bax A. Protein backbone angle restraints from searching adatabase for chemical shift and sequence homology. J BiomolNMR. 1999; 13:289–302.
39. Wang Z, Wang G. APD: the Antimicrobial Peptide Database. Nucleic Acids Res. 2004; 32:D590–D592. [PubMed: 14681488]
40. Wang G, Li X, Wang Z. APD2: the updated antimicrobial peptide database and its application in peptide design. Nucleic Acids Res. 2009; 37:D933–D937. [PubMed: 18957441]
41. Musale V, Casciaro B, Mangoni ML, Abdel-Wahab YHA, Flatt PR, Conlon JM. Assessment of the potential of temporin peptides from the frog Rana temporaria (Ranidae) as anti-diabetic agents. J Pept Sci. 2018; 24(2) in press. doi: 10.1002/psc.3065
42. Mangoni ML, Shai Y. Temporins and their synergism against Gram-negative bacteria and in lipopolysaccharide detoxification. Biochim Biophys Acta. 2009; 1788:1610–1619. [PubMed: 19422786]
43. Saravanan R, Joshi M, Mohanram H, Bhunia A, Mangoni ML, Bhattacharjya S. NMR structure of temporin-1 ta in lipopolysaccharide micelles: mechanistic insight into inactivation by outer membrane. PLoS One. 2013; 8:e72718. [PubMed: 24039798]
44. Ramarao N, Nielsen-Leroux C, Lereclus D. The insect Galleria mellonella as a powerful infection model to investigate bacterial pathogenesis. J Vis Exp. 2012; (70):e4392. [PubMed: 23271509]
45. Savini F, Luca V, Bocedi A, Massoud R, Park Y, Mangoni ML, Stella L. Cell-Density Dependence of Host-Defense Peptide Activity and Selectivity in the Presence of Host Cells. ACS Chem Biol. 2017; 12:52–56. [PubMed: 27935673]
46. Habash M, Reid G. Microbial biofilms: their development and significance for medical device-related infections. J Clin Pharmacol. 1999; 39:887–898. [PubMed: 10471979]
47. Ceri H, Olson ME, Stremick C, Read RR, Morck D, Buret A. The Calgary Biofilm Device: new technology for rapid determination of antibiotic susceptibilities of bacterial biofilms. J Clin Microbiol. 1999; 37:1771–1776. [PubMed: 10325322]
48. Mishra B, Wang G. Individual and combined effects of engineered peptides and antibiotics on the *Pseudomonas aeruginosa*biofilms. Pharmaceuticals. 2017; 10:58.
49. Wang G, Hanke ML, Mishra B, Lushnikova T, Heim CE, Chittezham Thomas V, Bayles KW, Kielian T. Transformation of human cathelicidin LL-37 into selective, stable, and potent antimicrobial compounds. ACS Chem Biol. 2014; 9:1997–2002. [PubMed: 25061850]
50. Wang G, Li Y, Li X. Correlation of three-dimensional structures with the antibacterial activity of a group of peptides designed based on a nontoxic bacterial mem brane anchor. J Biol Chem. 2005; 280:5803–5811. [PubMed: 15572363]
51. Koradi R, Billeter M, Wüthrich K. MOLMOL: a program for display and analysis of macromolecular structures. J Mol Graph. 1996; 14:51–55. [PubMed: 8744573]
52. Wang G. Structures of human host defense cathelicidin LL-37 and its smallest antimicrobial peptide KR-12 in lipid micelles. J Biol Chem. 2008; 283:32637–32643. [PubMed: 18818205]
53. Wang G, Mishra B, Epand RF, Epand RM. High-quality 3D structures shine light on antibacterial, anti-biofilm and antiviral activities of human cathelicidin LL-37 and its fragments. Biochim Biophys Acta. 2014; 1838:2160–2172. [PubMed: 24463069]
54. Mangoni ML. Temporins, anti-infective peptides with expanding properties. Cell Mol Life Sci. 2006; 63:1060–1069. [PubMed: 16572270]
55. Zasloff M. Magainins, a class of antimicrobial peptides from Xenopus skin: isolation, characterization of two active forms, and partial cDNA sequence of a precursor. Proc Natl Acad Sci U S A. 1987; 84:5449–5453. [PubMed: 3299384]

56. Wade D, Flock JI, Edlund C, Löfving-Arvholm I, Sällberg M, Bergman T, Silveira A, Unson C, Rollins-Smith L, Silberring J, Richardson M, Kuusela P, Lankinen H. Antibiotic properties of novel synthetic temporin A analogs and a cecropin A-temporin A hybrid peptide. Protein Pept Lett. 2002; 9:533–543. [PubMed: 12553862]

57. Rollins-Smith LA, Carey C, Conlon JM, Reinert LK, Doersam JK, Bergman T, Silberring J, Lankinen H, Wade D. Activities of temporin family peptides against the chytrid fungus (Batrachochytrium dendrobatidis) associated with global amphibian declines. Antimicrob Agents Chemother. 2003; 47:1157–1160. [PubMed: 12604562]

58. Abbassi F, Galanth C, Amiche M, Saito K, Piesse C, Zargarian L, Hani K, Nicolas P, Lequin O, Ladram A. Solution structure and model membrane interactions of temporins-SH, antimicrobial peptides from amphibian skin. A NMR spectroscopy and differential scanning calorimetry study. Biochemistry. 2008; 47:10513–10525. [PubMed: 18795798]

59. Wang X, Wang G. Insights into Antimicrobial Peptides from Spiders and Scorpions. Protein Pept Lett. 2016; 23:707–721. [PubMed: 27165405]

Highlights

- Antimicrobial, antifungal and anticancer activities of six temporins were characterized;
- Temporin-1OLa with a better cell selectivity was antibiofilm in vitro and anti-staph infection in vivo;
- Three-dimensional structure of temporin-1Ola, determined by the improved 2D NMR method, revealed a hydrophobic patch followed by a short two turn-helix;
- Bioinformatic analysis of temporins led to six models and confers significance to temporin-1OLa.

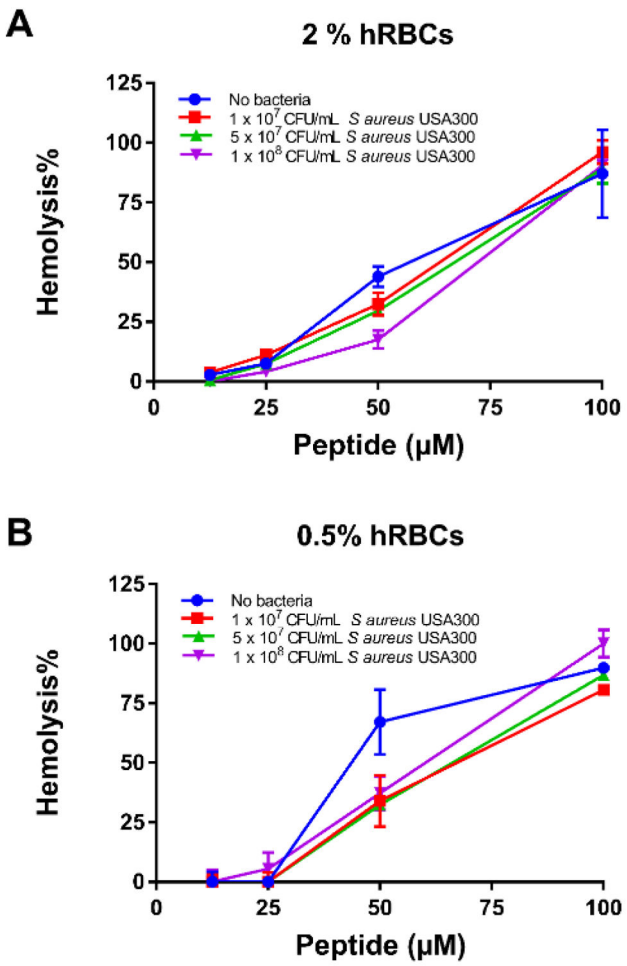

Fig. 1.

Hemolytic activity of Temporin-1OLa in the absence and presence of *S. aureus* USA300. Human erythrocytes were incubated with varying amounts of bacterial cells and peptide for one hour.

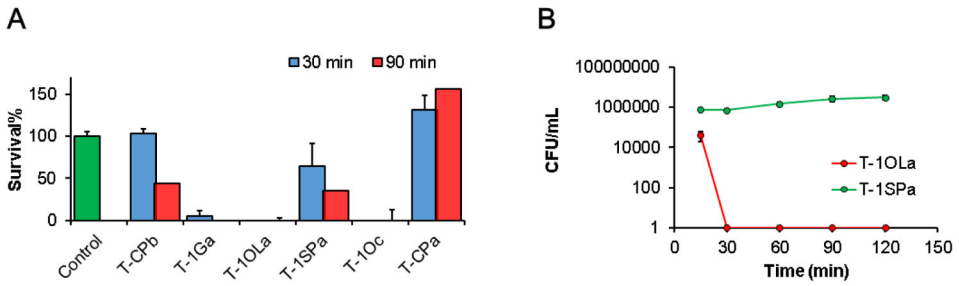

Fig. 2.

Killing kinetics of *S. aureus* USA300 after treatment with 3.1 μM peptide. (A) Survival rates of *S. aureus* after 30 min (blue bars) or 90 min (red) killing by the six temporins. The control (green) was not treated with any peptide. (B) Time-dependent killing of *S. aureus* by temporin-1OLa and temporin-1SPa.

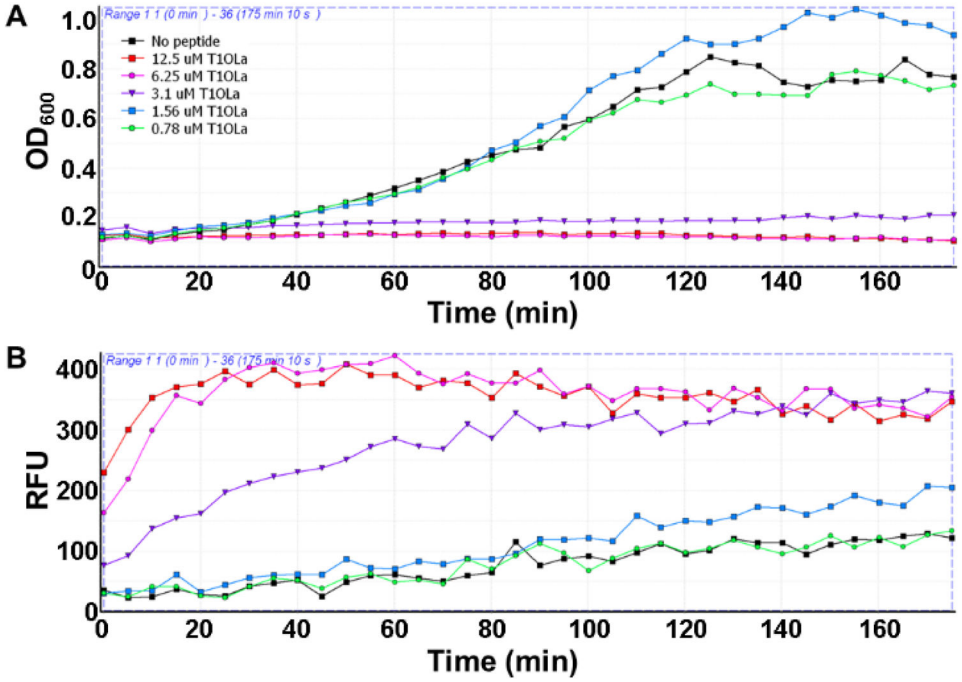

Fig. 3.

Simultaneous detection of bacterial growth inhibition (A) and membrane damage (B) by absorbance (OD_{600}) and fluorescence spectroscopy of *S. aureus* USA300 by temporin-1OLa at various concentrations. RFU: relative fluorescence units.

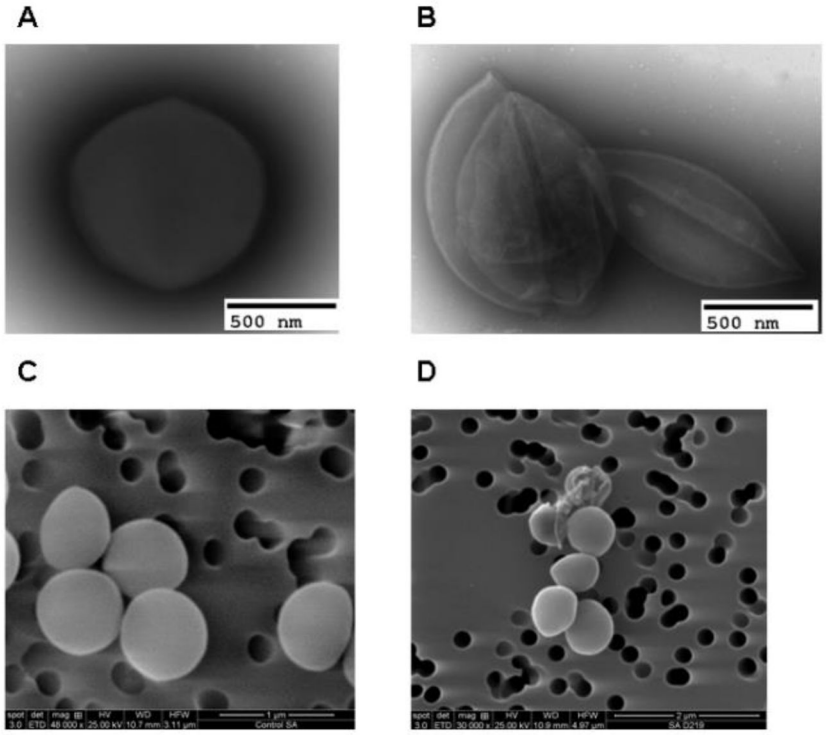

Fig. 4.

Electron microscopic (EM) images of *S. aureus* USA300 with and without treatment with temporin-1OLa. The top two panels are transmission EM with negative staining for control (A) and treated with 25 μM temporin-1OLa (B) and the bottom two panels are scanning EM for the control (C) and the peptide treated at 6.25 μM (D).

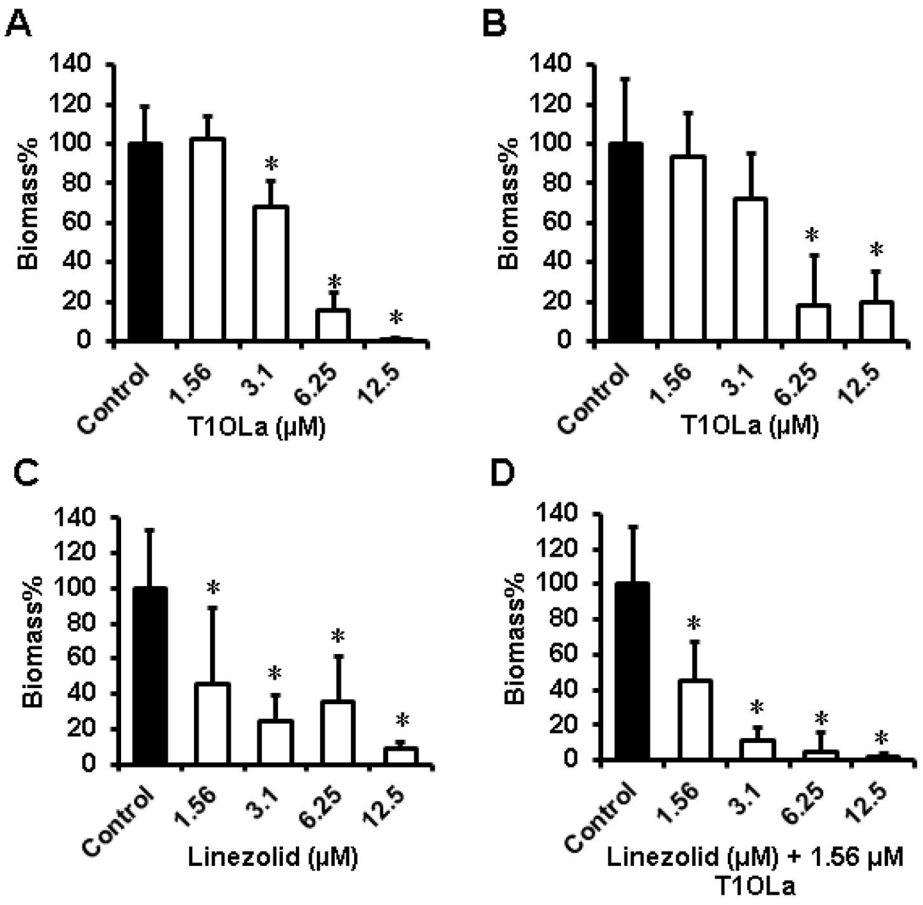

Fig. 5.

Antibiofilm activity of temporin-1OLa (T1OLa) alone and in combination with linezolid against *S. aureus* USA300: (A) Inhibition of biofilm formation by 10^8 CFU/mL initial bacterial load; (B) Disruption of 24 h established biofilms by temporin-1OLa; (C) Disruption of 24 h established biofilms by linezolid; and (D) Disruption of 24 h established biofilms by linezolid in the presence of 1.56 μM

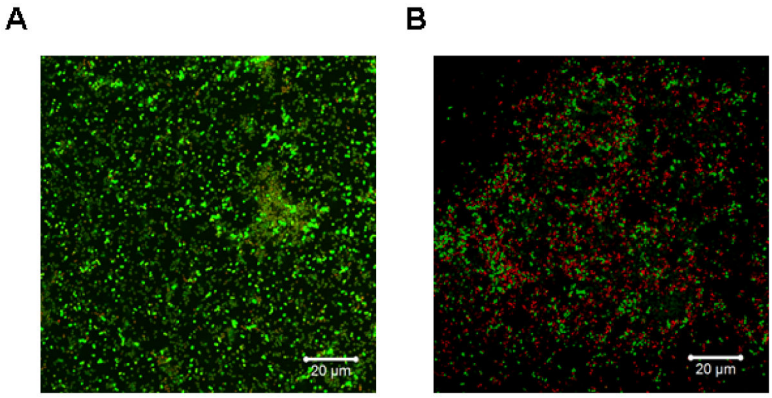

Fig. 6.

Confocal laser scanning micrographs of 24 h control biofilm (A) and treated with 12.5 μM temporin-1OLa (B). Biofilms were stained with the live and dead cell staining kit, which uses SYTO-9 (green) for live cells and propidium iodide (red) for dead cells.

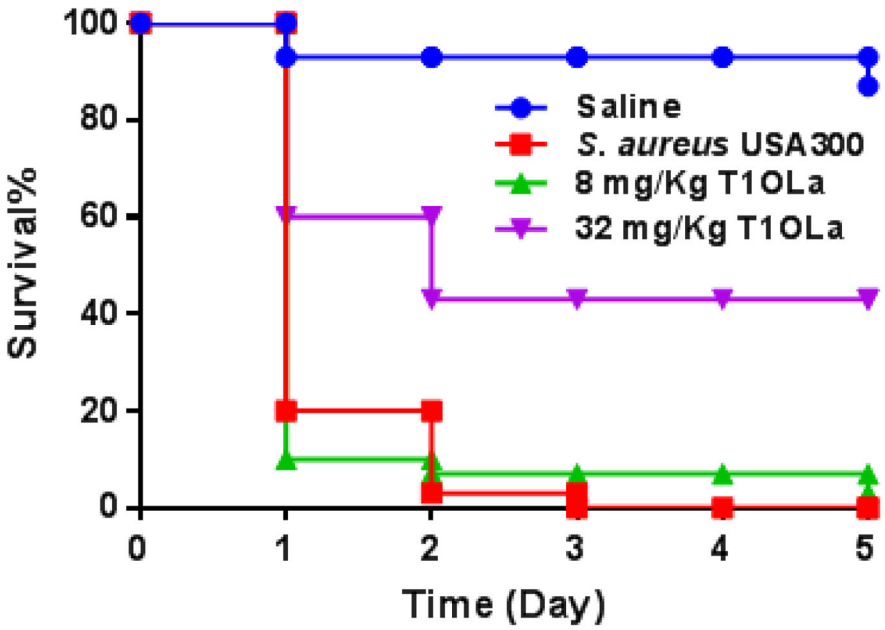

Fig. 7.

Survival of wax moths under different conditions: blue line, treated with saline only; purple line, treated with 32 mg/kg temporin-1OLa (T1OLa) and 2h later infected with 1×10^6 CFU *S. aureus* USA300; green line, treated with 8 mg/kg T1OLa and 2h later infected with 1×10^6 CFU *S. aureus* USA300; red line, infected with 1×10^6 CFU *S. aureus* USA300 only.

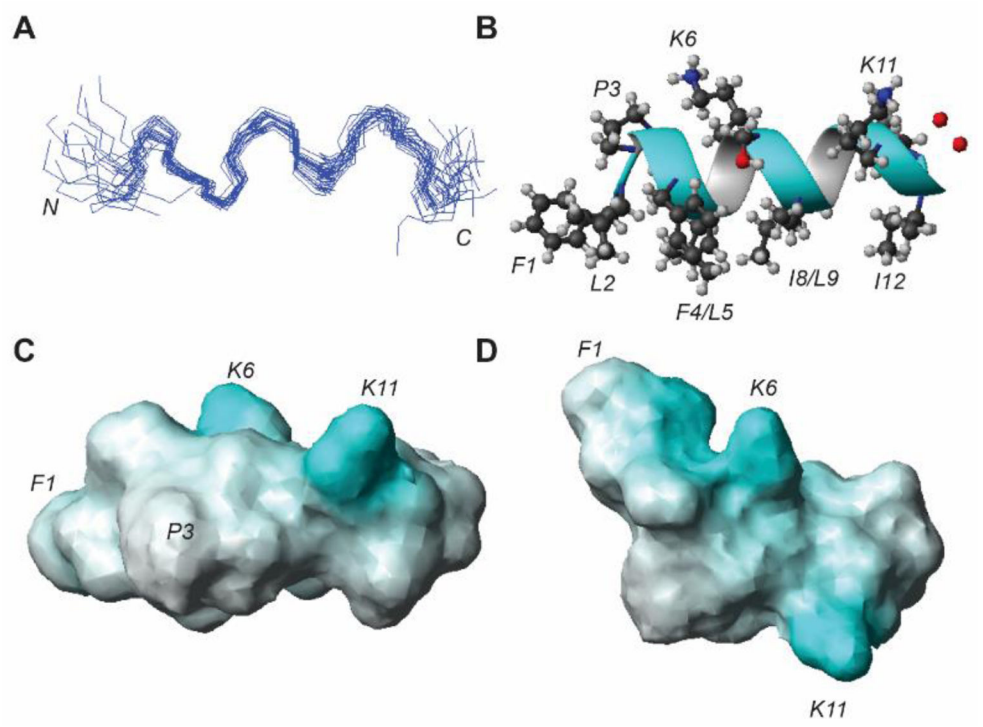

Fig. 8.

NMR structure of temporin-1OLa bound to membrane-mimetic deuterated SDS micelles (peptide:SDS molar ratio of 1:60) at pH 5.6 and 35°C. Shown are (A) an ensemble of superimposed 20 backbone structures, (B) a ribbon diagram with sidechain displayed, (C) the potential surface and its another view after a 90° rotation.

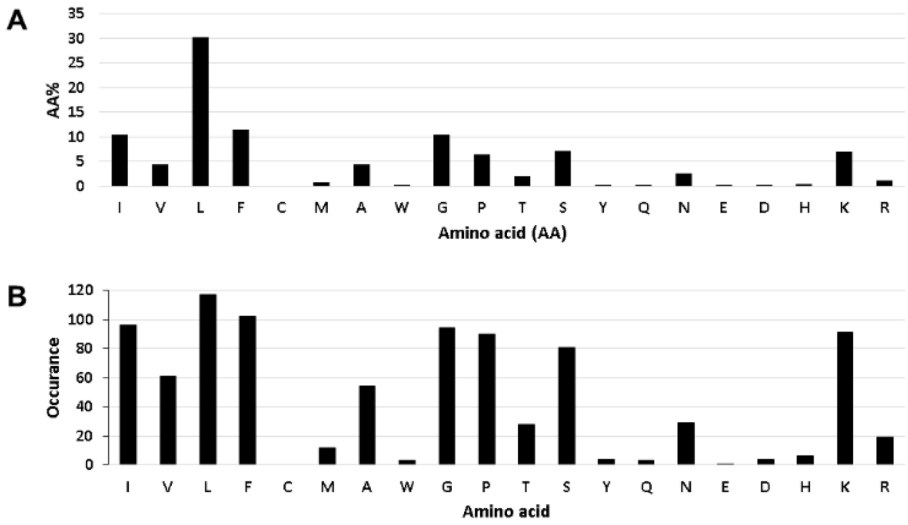

Fig. 9.

Bioinformatic analysis of temporins in the antimicrobial peptide database (see Methods): (A) averaged content for each amino acid in all temporins and (B) frequency of each amino acid in temporins (i.e., the number of temporins that use each amino acid). Accessed March 30, 2018.

Table 1

Peptides and Calculated Parameters

Temporin	APD ID[a]	Sequence	Net charge	FL IV	Pho%	PG	Boman Index	Ref
CPb	1497	FL**P**IVGRLISGIL	2	8	61	1P2G	−1.54	22
1Ga	823	SIL**P**TIVSFLSKVF	2	8	57	1P	−1.09	23
1OLa	871	FL**P**FLKSILGKIL	3	8	61	1P1G	−1.68	24
1SPa	1444	FLSAITSILGKFF	2	7	61	1G	−1.26	25
1Oc	819	FL**P**LLASLFSRLF	2	8	69	1P	−1.04	26
CPa	1496	I**PP**FIKKVLTTVF	3	7	53	2P	−0.96	22

[a]Additional information can be found in the antimicrobial peptide database (APD) and references. Peptide net charge, hydrophobic content (Pho%), the sum of amino acids FLIV or PG, and Boman index were calculated using the APD tool [10].

Table 2

Antibacterial Activity and Hemolytic Ability of Various Temporin Peptides

Temporin	MIC (μM)[1]						HL_{50} (μM)	t_R[2] (min)	CSI
	SA	SE	BS	EC	KP	PA			
CPb	12.5	12.5	25–50	>50	>50	>50	>100	13.711	>8
1Ga	3.1	3.1	6.3	>50	>50	>50	12.5	16.498	4
1OLa	1.6–3.1		12.5–25	>50	50	>50	50	14.129	16–32
1SPa	6.3	6.3	12.5	>50	>50	>50	37.5	14.399	6
1Oc	1.6	1.6	12.5	>50	>50	>50	<12.5	15.628	<8
CPa	≥25	12.5	50	12.5	50	>50	>100	14.036	~4
Vancomycin	0.78	1.6	>3.1	>50	>50	>50	NA	NA	NA

[1] SA, Staphylococcus aureus USA300; SE, Staphylococcus epidermidis; BS, Bacillus subtilis 168; EC, Escherichia coli ATCC 25922: KP, Klebsiella pneumoniae ATCC13883; PA, Pseudomonas aeruginosa PAO1;

[2] t_R, the retention time of the peptide on a reverse-phase HPLC; CSI, cell selectivity index; NA, not available.

Table 3

Antifungal and Anticancer Activities of the Six Temporin Peptides

Temporin	MIC (μM)			LC_{50} (μM)		
	C. albicans	*C. glabrata*	*C. tropicalis*	4T1[1]	HeLa	HaCaT
CPb	50	>50	6.2–12.5	>80	>80	>200
1Ga	12.5	12.5	3.1	20	>80	40
1OLa	12.5	12.5	1.6	>80	25	100
1SPa	25	25	6.2	>80	>80	200
1Oc	25	25	1.6–3.1	65	50	50
CPa	25	12.5	3.1–6.2	80	>80	100

[1] Mouse breast cancer cells 4T1.

Peptides. Author manuscript; available in PMC 2019 August 01.

Table 4

Effects of Salts, pH, and Serum on Anti-staphylococcal Activity of Temporin-1OLa

Condition	pH 8	pH 7.4	pH 6.8	150 mM NaCl	5% serum	10% serum
Peptide MIC	3.1	3.1	6.2	3.1	12.5	25

Table 5

Proline-based Classification of Natural Temporins and Model Abundance (%) in the Antimicrobial Peptide Database[10]

Model	Representative sequence pattern	APD ID	Temporin	P #	N-end	C-end	Peptide count	%
1	*FVQWFS*KF*L*GR*IL*	101	L	0	0	0	31	25.6%
2	*FL***P***FL*KS*IL*GK*IL*	871	1OLa	1	1	0	75	62.0%
3	***/PP****FI*KK*VL*TT*VF*	1496	CPa	2	2	0	4	3.4%
4	*FF*GS*VL*K*L***/P**K*IL*	1434	PTa	1	0	1	1	0.8%
5	S*L*SR*FL*S*FL*K*IVY***PP****AF*	1348	LTc	2	0	2	1	0.8%
6	*FL***P***IAL*K*AL*GS*IF***P**K*IL*	1448	LT2	2	1	1	9	7.4%